JULY 1980

Ph. 1521

PPPL-1675

UC-20g

THEORY OF DRIFT, TRAPPED-PARTICLE, AND ALFVÉN INSTABILITIES AND ANOMALOUS PLASMA TRANSPORT

PLASMA PHYSICS LABORATORY

PRINCETON UNIVERSITY
PRINCETON, NEW JERSEY

This work was supported by the U.S. Department of Energy Contract No. DE-AC02-76-CHO 3073. Reproduction, translation, publication, use and disposal, in whole or in part, by or for the United States government is permitted.

THEORY OF DRIFT, TRAPPED-PARTICLE, AND ALFVÉN INSTABILITIES AND ANOMALOUS PLASMA TRANSPORT

by

L. Chen, M. S. Chance, C. Z. Cheng, E. A. Frieman, P. K. Kaw,
W. W. Lee, H. Okuda, G. Rewoldt, P. H. Rutherford, W. M. Tang,

Princeton University, Plasma Physics Laboratory
Princeton, N.J. 08544

P. N. Guzdar, Y. C. Lee, R. Marchand

Universtity of Maryland, College Park, Maryland

W. M. Nevins

Lawrence Livermore Laboratory, University of California,
Livermore, California

K. T. Tsang, D. J. Sigmar, J. C. Whitson

Oak Ridge National Laboratory
Oak Ridge, Tennessee

PPPL-1675 July 1980

Presented at the 8th International Conference on Plasma Physics and Controlled Nuclear Fusion Research, Brussels, Belgium, 1-10 July 1980.

Theory of Drift, Trapped-Particle, and Alfvén Instabilities and Anomalous Plasma Transport

ABSTRACT

In Part A, we present results of theoretical investigations on the linear and nonlinear aspects of microscopic low-frequency drift, trapped-particle, and shear-Alfvén instabilities in systems with finite magnetic shear. The investigations employ analytical and numerical methods, and also particle simulations. In particular, the following subjects are considered: (1) stability of drift-wave eigenmodes in a sheared slab geometry including finite ion-temperature gradients; (2) instabilities in the neutral-beam-heated PLT; (3) application of the ballooning-mode formalism to drift, trapped-electron and shear-Alfvén instabilities in toroidal geometry; and (4) nonlinear interactions of drift and drift-Alfvén waves and associated anomalous transport.

In Part B, we show that finite ion-Larmor-radius effects can remove the shear-Alfvén continuous spectrum extensively discussed in ideal magnetohydrodynamic (MHD) theories. In the absence of free energy or dissipation, the resultant eigenmodes are discrete and neutrally stable. Toroidal drifts of alpha (or energetic) particles are found to destabilize these modes. Stability studies of the parametric variations of the energy and density scale lengths of the energetic particles show that, even in the presence of electron Landau damping, modes with low radial mode numbers remain unstable in most cases. Since alpha particles are concentrated in the center of the plasma, this drift-type instability may imply anomalous He-ash removal.

1. PART A. DRIFT, TRAPPED-PARTICLE, AND ALFVÉN INSTABILITIES AND ANOMALOUS PLASMA TRANSPORT

By L. Chen, M. S. Chance, C. Z. Cheng, E. A. Frieman, P. N. Guzdar, Y. C. Lee, R. Marchand, W. M. Nevins, P. K. Kaw, W. W. Lee, H. Okuda, G. Rewoldt, P. H. Rutherford, W. M. Tang

1.1 Stability of Drift Modes in Sheared-Slab Geometries

Recently, stability analyses of the collisionless (universal) drift mode have been generalized to the case of arbitrary radial wavelengths; where the eigenmodes are described by the following integral equation ,

$$\int_{-\infty}^{\infty} dk_x' \left[(\tau + 1/\Omega)\, \overline{\xi_i Z_i}(k_x' - k_x)\, \sigma(k_x') + (1 - 1/\Omega)\right.$$

$$\left. \overline{\xi_e Z_e}(k_x - k_x')\right] \bar{\phi}(k_x') + \bar{\phi}(k_x) = 0 \,, \qquad (1)$$

where $\tau \equiv T_e/T_i$, $\Omega \equiv \omega/\omega_{*e}$, $\omega_{*e} = k_y T_e c/eBL_n$, $\xi_j = \omega/|k_{||}' x|v_{tj}$, $k_{||}' = k_y/L_s$, $Z_j = Z(\xi_j)$, Z is the plasma dispersion function, L_n and L_s are, respectively, density and magnetic shear scale lengths, $\sigma(k_x) = I_o(b_i)\exp(-b_i)$, $b_i = \rho_i^2(k_x^2 + k_y^2)/2$, I_o is the modified Bessel function, and

$$\bar{A}(k_x) = (1/2\pi)\int_{-\infty}^{\infty} dx\, A(x)\exp(-ik_x x).$$

Both analytical [1] and numerical [2] treatments of Eq. (1) have shown that, as in the differential-equation approximation, the eigenmodes are stable. While Eq. (1) is widely accepted, a closer examination of its derivation reveals that it is in error due to the assumption that the spatial dependence due to the parallel wave number $k_{||}$ is weakly varying, which is generally not true near the mode-rational surface. In fact, the correct equation has been derived by Coppi, Rosenbluth, and Sagdeev [3], and can be cast in the form of Eq. (1) with σ replaced by

$$\tilde{\sigma}(k_x, k_x') = I_o(\bar{b}_i)\exp(-\hat{b}_i), \qquad (2)$$

where $\bar{b}_i = [(k_x^2 + k_y^2)(k_x'^2 + k_y^2)]^{1/2}\rho_i^2/2$ and $\hat{b}_i = (k_x^2 + k_x'^2 + 2k_y^2)\rho_i^2/4$. A stability proof, similar to that in Ref. [1], can be carried out for the correct equation to show that, again, the eigenmodes are always stable. The same conclusion is also obtained numerically [4].

The stability of the universal eigenmode, however, is tied to the even symmetry of electron velocity distribution $F_{oe}(v_{||}) = F_{oe}(|v_{||}|)$ and, thus, for asymmetric $F_{oe}(v_{||})$, the eigenmode can become unstable [5]. To illustrate this point, we consider the following $F_{oe}(v_{||})$

$$F_{oe}(v_{||}) = \begin{cases} C_1/(1 + v_{||}^2/v_e^2)^2, & \text{for } v_{||} > 0 \\ C_1/(1 + v_{||}^2 R^2/v_e^2)^n, & \text{for } v_{||} < 0; \end{cases} \qquad (3)$$

where $C_1 = 4/v_e\pi[1 + 2(2n - 3)!!/R(2n - 2)!!]$ and $R = (n-1)^{-1/2}$ to ensure $\int F_{oe}\, dv_{||} = 1$ and $\int v_{||}\, F_{oe}\, dv_{||} = 0$. If the asymmetry is strong ($n \gg 2$), the eigenmode is found to be highly localized away from the mode-rational surface and, therefore, a parabolic approximation of the eigenmode potential can be made. We then derive the following instability growth rate

$$\mathrm{Im}\Omega \simeq \sqrt{3}\,\{-L_n/L_s + 2^{-1/3}\,\Omega_o[1 + (L_n/2\Omega_o L_s)^{1/3}][(m_e/m_i)(1/\Omega_o - 1)^2]^{1/3}\}, \qquad (4)$$

$\Omega_o \simeq 1/(1 + b_s)$, and $b_s = k_y^2\tau\rho_i^2/2$. Thus, the eigenmode becomes unstable for sufficiently weak shear in agreement with the numerical results. It, therefore, suggests that, in realistic situations, a detailed knowledge of $F_{oe}(v_{||})$ may be crucial in determining the stability of the universal eigenmode.

The enhanced density fluctuations observed in the neutral-beam-heated PLT [6] have stimulated much interest in the effects of finite ion-temperature gradients

[$\eta_i \equiv (d\ln T_i/dx/d\ln N/dx) \neq 0$] on drift modes [7]. To demonstrate the finite-η_i effects, let us consider a sheared slab and assume adiabatic (Boltzman) electrons, fluid ions, and the small ion-Larmor-radius approximation. For $|\eta_i| >> 1$, the eigenmode equation can be readily solved and, for $|b_s\eta_i| < \tau$ and the lowest eigenstate, we obtain the following two branches from the dispersion relation:

$$\Omega_1 \approx i\,\eta_i\, L_n/L_s\tau \quad , \tag{5}$$

and $$\Omega_2 \approx [1 - i(1 + \eta_i/\tau)\, L_n/L_s]/(1 + b_s) \quad . \tag{6}$$

Ω_1 corresponds to the ion diamagnetic drift mode destabilized by positive η_i; this is the usual (positive) η_i instability [3]. A threshold value, $\eta_i^+ \approx 1$, appears when ion kinetic effects are kept [8]. Ω_2, on the other hand, corresponds to the electron drift mode. For $\eta_i = 0$, Ω_2 reduces to the familiar Pearlstein-Berk result [9]. Equation (6) thus indicates positive (negative) η_i's enhance (reduce) the shear-damping rate and, for $\eta_i \leq \eta_i^- \approx -\tau$, a new negative η_i instability. These predictions have been verified by numerical solutions of the eigenmode equation which includes both ion kinetic and nonadiabatic electron responses.

1.2 Instabilities in the Neutral-Beam-Heated PLT

In order to describe the instabilities more realistically, we have developed a radially local code which contains the essential physics of the trapped-ion, the trapped-electron and the positive-η_i drift modes and employs equilibrium profiles obtained from a one-dimensional radial transport code [10] modeling the neutral-beam-heated PLT. In particular, the equilibrium density and temperature for electrons, hydrogen, deuterium, and carbon, and the safety factor q, together with their derivatives, were evaluated halfway between mode-rational surfaces at $r \approx 22$ cm., the center radius of the microwave scattering volume for density fluctuations. For a toroidal mode number $\ell = 30$, the mode goes unstable when $T_i(r = 0) \approx 2.3$ keV (where $T_i = T_H \approx T_D \approx T_C$). The instability has a characteristic frequency (in the ion diamagnetic direction) of the order of the ion bounce and transit frequencies and, therefore, can be regarded as a hybrid of the trapped-ion, trapped-electron, and ion-temperature-gradient modes. When compared with the experimentally observed threshold, $T_i(r \approx 0) \approx 3$-4 keV, it can be concluded that there is agreement within the accuracy of the input equilibrium quantities at $r \approx 22$ cm. Hence, this suggests the possibility that, below the threshold (which is a combined threshold mainly on T_i and η_i at $r \approx 22$ cm.), there is a weakly unstable (trapped-electron, drift) mode saturated at a low level, and that, when the threshold is exceeded, the hybrid mode goes unstable with a much higher growth rate. If this stronger instability saturates at a higher level, it could give rise to the sudden increase in the fluctuation level observed in PLT.

1.3 Drift, Trapped-Electron, and Shear-Alfvén Instabilities in Toroidal Geometries

Recently, the ballooning-mode formalism, first developed for ideal MHD ballooning modes, has been generalized to low-frequency kinetic microinstabilities [11]. Employing this formalism, significant new understanding has been gained on the stability of drift-type modes in tokamaks. In particular, it is found that, due to the appearance of a new eigenmode branch due entirely to the finite toroidal coupling, the stability properties can be qualitatively different from those predicted using the slab model.

Let us consider an axisymmetric tokamak with concentric, circular magnetic surfaces. For simplicity, we further assume cold ions, and suppress electron dissipation in order to concentrate on the shear-damping effect. In the ballooning-mode representation, the corresponding (electrostatic) eigenmode equation is [11, 12]

$$[d^2/d\hat{\theta}^2 + \eta_s^2 \Omega^2 \quad Q(\Omega,\hat{\theta})]\ \hat{\phi}\ (\hat{\theta}) = 0; \quad -\infty < \hat{\theta} < \infty \tag{7}$$

where

$$Q = b_s(1 + \hat{s}^2\ \hat{\theta}^2) + 1 - 1/\Omega + (2\epsilon_n/\Omega)\ (\cos\hat{\theta} + \hat{s}\ \hat{\theta}\ \sin\hat{\theta}), \tag{8}$$

$\eta_s^2 = b_s q^2/\epsilon_n^2$, $\hat{s} = r\,q'/q$, $\epsilon_n = r_n/R$, $r_n^{-1} = |d\ln N(r)/dr|$, and θ can be regarded as the coordinate along the magnetic field line. In deriving Eq. (7), we also assume that there is no radial phase shift between modes located at neighboring mode-rational surfaces. Equation (7) shows that toroidal coupling has the effect of modulating the otherwise "anti-well" potential structure and, thereby, introducing local potential wells. Numerical solutions of Eq. (7) have identified two eigenmode branches. One is the usual slab-like (Pearlstein-Berk) eigenmode branch, and the other is the new toroidicity-induced branch. The slab-like branch, just as in the slab model, has "anti-well" potential structure. The eigenmodes, hence, are unbounded and experience finite shear damping. The toroidicity-induced branch, however, has negligible shear damping since its eigenmodes are quasi-bounded by the local wells. For the universal drift mode, we find, both analytically and numerically, that the eigenmodes of the toroidicity-induced branch can be destabilized by either collisional [13] or collisionless [14] electron dissipation, contrary to slab-model predictions; while the slab-like ones always remain stable. Calculations have also been done for the trapped-electron mode [15], and the results show that the toroidicity-induced branch is much more unstable than the slab-like branch. As for the positive-η_i drift mode, it is found that for $\eta_i > 1$, the unstable eigenmodes are strongly ballooning and toroidal coupling further destabilizes the instability [16].

The success of the ballooning-mode formalism in treating tokamak microinstabilities has stimulated several extensions of the calculation. First, a more general ion response is employed which is valid for both trapped-electron and trapped-ion regimes, and for arbitrary ratios of the perpendicular wavelength to the ion Larmor radius and banana width. Second,

a fully electromagnetic analysis has been carried out by including the parallel ($\hat{A}_{\parallel}$) and perpendicular components ($\hat{A}_{\perp}$) of the vector potential along with the electrostatic potential $\hat{\phi}$ in the ballooning-mode formalism, so that the eigenmodes of the shear-Alfvén as well as the finite-β ($\beta \equiv$ plasma pressure/magnetic pressure) modified drift branches can be investigated. (We note that the MHD ballooning mode belongs to the shear-Alfvén branch.) In Figure 1, we show $\omega = \omega_r + i\gamma$ versus β for eigenmodes in both branches. The parameters used here are $\epsilon_0 = r/R_0 = 0.1$, $T_e = 1$ keV, $T_i = 0.5$ keV, $q = 2.5$, $q'r/q = 1$, $r_n/r = 1$, $m_i/m_e = 3672$, $\nu_e^* = 0.03$, and $b_{i\theta} = 0.2$ (or $k_\theta \rho_i = 0.63$). Figure 1 (b) corresponds to the lowest eigenstate of the drift branch for $\eta_i = \eta_e = 0$. It can be seen that increasing β has a significant effect only for $\beta \gtrsim 1\%$. The eigenfunction here has $\hat{\phi}(\hat{\theta})$ and $\hat{A}_{\perp}(\hat{\theta})$ even and $\hat{A}_{\parallel}(\hat{\theta})$ odd. A perturbative analysis, valid for $\beta \lesssim \epsilon^2 \sim 1\%$, reveals that the numerical results presented here correspond to the toroidicity-induced eigenmode branch whose stability is little affected by the finite-β coupling to the shear-Alfvén branch. The slab-like branch, however, is found to be further stabilized due to enhancement in its shear-damping rate. Figure 1 (a) shows ω versus β for the shear-Alfvén branch with $\hat{\phi}(\hat{\theta})$ odd and $\hat{A}_{\parallel}(\hat{\theta})$ even and for $\eta_i = \eta_e = -1$; (negative η's are destabilizing for this mode). Here, the growth rate increases rapidly above a critical β value and then saturates. For both branches, the effect of including $\hat{A}_{\perp}$ in the calculation is small even for $\beta \approx 10\%$. However, the MHD equilibrium used here is frozen, with circular, concentric magnetic surfaces. With more realistic MHD equilibria, it is not expected that this will remain true for these large β values. Hence, results for γ and ω_r shown in Fig. 1 are somewhat artificial in this sense.

1.4 Drift and Drift-Alfvén Turbulence and Anomalous Transport

The linear gyrokinetic formalism has been extended to the nonlinear regime using the following unified ordering scheme

$$\frac{\delta f}{F} \sim \frac{e\delta\phi}{T} \sim \frac{\delta n}{N} \sim \frac{\delta b}{B} \sim \frac{\omega}{\Omega_i} \sim \frac{k_\parallel}{k_\perp} \sim \frac{1}{k_\perp a} \sim \frac{\rho_i}{a} \sim \delta \ll 1 .$$

A system of equations can then be self-consistently derived for the nonlinear evolution of both microscopic and macroscopic quantities. The formalism has the advantages of being valid for (1) $k_\perp \rho_i \sim O(1)$, (2) arbitrary β values, (3) the strong turbulence regime where nonlinear time scales $\sim$ linear time scales $\sim O(\omega_*^{-1})$, (4) realistic geometries and, therefore, is adaptable to the ballooning-mode representation. As a simple application of this formalism, we show that, for drift as well as drift-Alfvén waves, the spectral energy transfer due to the ion-induced scattering is from short to long perpendicular wavelengths. Meanwhile, numerical studies of three nonlinearly interacting drift waves, $(\omega_j, \underline{k}_j)$ for $j = 1, 2, 3$, have shown that the nonlinear dynamics can be strongly modified by the $\delta\underline{E} \times \underline{B}\cdot\nabla\delta n \propto \Gamma(k_j)$ nonlinearity in addition to the ion polarization drift nonlinearity considered by Hasegawa and Kodama [17]. Here $\Gamma(k_j)$ is the growth ($\Gamma > 0$) or damping ($\Gamma < 0$) rate corresponding to the nonadiabatic electron response. Specifically, for $k_1 < k_2 < k_3$, $\Gamma(k_1)$, $\Gamma(k_2) \geq 0$, and $\Gamma(k_3) \leq 0$, the results are (1) for

$\Gamma(k_1)=0$, the ion polarization drift is the only nonlinearity and, as predicted Ref. 17, more energy is transferred to the k_1 mode than to the k_3 mode; (ii) for $\Gamma(k_1)$, $\Gamma(k_2) > 0$, $\Gamma(k_3) < 0$ and keeping only the nonlinear ion polarization drift, no steady state is reached; and (iii) inclusion of the $\delta\tilde{E} \times \tilde{B}\cdot\nabla\delta n$ nonlinearity leads to bounded solutions for the three-wave interaction. However, a significant damping rate $|\Gamma(k_3)/\omega_3| \sim O(10^{-1})$, is needed to achieve a steady state.

The η_i drift instability in a sheared slab and its nonlinear evolution have been simulated using a two-and-half dimensional (2-1/2D) particle code. For $\eta_i > \eta_c^+$, the observed characteristics of the linear instability agree well with those predicted from an eigenmode analysis. The nonlinear phase of the instability is accompanied by a large ion thermal transport which flattens the ion temperature profile and, thereby, leads to saturation. For $\eta_i \lesssim \eta_c^+$, enhanced fluctuations due to marginally stable modes have also been observed. In both cases, fluctuation amplitudes and, hence, the resulting anomalous transport are found to depend critically on the linear eigenmode widths. Furthermore, the observed thermal conductivities are much larger than those predicted from a local quasi-linear theory.

A 2-1/2D simulation has also been carried out to investigate microscopic shear-Alfvén eigenmodes of the tearing-mode parity. While the eigenmodes are linearly stable, it is observed that fluctuations associated with the lowest eigenmode are enhanced over the thermal level and a quasi-linear modification of the zeroth-order current is observed near the mode-rational surface. The observed steady state is characterized by the nullification of the zeroth-order current and shear, as well as rapid electron radial energy transport near the mode-rational surface due to the formation of microscopic magnetic islands.

Finally, we examine the interesting phenomenon observed in the shearless layer of a multipole: that while large-amplitude low-frequency density fluctuations ($\delta n/N \lesssim 30\%$) can be completely quenched when the safety factor q is a rational number, the plasma confinement has actually deteriorated in this case by 50% [18]. It is believed that these observations for rational q values can be explained in terms of nonlinear excitation of convective cells and, consequently, enhanced particle diffusion by drift-wave instabilities [19]. Specifically, once convective cells are nonlinearly excited to amplitudes comparable to drift-waves, the drift instabilities are quenched due to the phase-mixing of particle orbits. Meanwhile, since convective cells are incompressible, the associated density fluctuations are small [20], which is consistent with the observation. For irrational q values, however, the convective cells are strongly damped since the field lines are not closed. Furthermore, for $k_\perp\rho_i < 1$, the mode-coupling coefficients of drift waves are small and, hence, drift modes saturate at high amplitudes. Numerical simulations using a three-dimensional cylindrical particle code have been performed to verify the theoretical interpretations described. The simulation parameters are $m_i/m_e = 400$, $T_e/T_i = 16$, $\Omega_e/\omega_{pe} = 4$, a 64 x 64 two-dimensional spatial

grid, $\rho_1 = 2$, $\underset{\sim}{B} = B_z \underset{\sim}{e}_z + B_p(r)\, \underset{\sim}{e}_\theta$, L_z (system length in z) = 640 and 4 ~ 5 Fourier modes are employed to represent z-direction variations. Also, $B_p(r) \propto r$ so that $q \equiv 2\pi r\, B_z/B_p(r)$ is constant, i.e., there is no shear. Runs have been made with $q = 2$ and $\sqrt{5}$, respectively, to study the q-value effects on the density fluctuations. Furthermore, in order to model the experiments more closely, steady-state simulations have been carried out with the initial density and temperature profiles more or less maintained. Figure 2 shows the time development of the potential fluctuations for several modes when the q value is irrational, i.e., $q = \sqrt{5}$ and, in this case, there is no convective cell. It is clearly seen that several drift modes, (m,n) = (-1,0), (-4,2), (-3,1) remain at large amplitudes even after saturation. Figure 3 shows the case of $q = 2$ with the other parameters kept fixed. Here, it is seen that the drift modes, (m,n) = (-1,1) and (-3,1) first grow to large amplitudes at $t = 2400\ \omega_{pe}^{-1}$ and then decay away to small amplitudes. Meanwhile, convective cells (m,n) = (-2,1), grow slowly and saturate at a level comparable to the drift waves. The saturation level here is quite small compared with the $q = \sqrt{5}$ case, which is consistent with experimental results.

PART B

Destabilization of Low Mode Number Alfven Modes in Tokamaks by Energetic Beam or Alpha Particles

K. T. Tsang, D. J. Sigmar, and J. C. Whitson
Oak Ridge National Laboratory
Oak Ridge, Tennessee 37830, U.S.A.

With the inclusion of finite Larmor radius effects, the second order differential equation for the ideal MHD Alfven wave is replaced by a fourth order one [21,22]. Discrete eigensolutions are possible because the Alfven singularity is removed from the highest derivative. Rosenbluth and Rutherford first included this fourth order finite Larmor radius term to investigate the excitation of shear Alfven waves by energetic ions in a tokamak. However, the fourth order term they derived is valid only in slab geometry for rather short radial wave lengths. In cylindrical geometry, their slab fourth order term is incompatible with the boundary condition at $r = 0$, where r is the minor radius. Therefore if one uses the Rosenbluth-Rutherford equation in cylindrical geometry, a global unstable mode can be found even when the energetic ion contribution is turned off, clearly a spurious result.

We give the correct fourth order eigenmode equation in cylindrical geometry and construct a quadratic form to show that the eigenmodes are always neutrally stable in the absence of free energy and dissipation. The effect of alpha particles manifests itself predominantly through the current due to their large toroidal drift motion. The electrons contribute a stabilizing Landau resonance through the charge neutrality condition. Charge neutrality and Ampere's law provide two equations for the scalar and vector potentials (ϕ, $A_\parallel$). There results a single fourth order eigenmode equation for cylindrical geometry

$$\rho_i^2 \left[\frac{1}{r^2}\frac{\partial}{\partial r} U_1 r^3 \frac{\partial}{\partial r}\frac{1}{r} - \frac{m^2-1}{r^2} U_1\right]\cdot\left(\frac{1}{r}\frac{\partial}{\partial r} r \frac{\partial}{\partial r} - \frac{m^2}{r^2}\right)\phi$$

$$+ \frac{1}{r^2}\frac{\partial}{\partial r} r^3 U_0 \frac{\partial}{\partial r}\frac{\phi}{r} - \frac{m^2-1}{r^2} U_0 \phi = 0, \qquad (9a)$$

where

$$U_0 = \omega^2/v_A^2 - k_\parallel^2 - \beta_\alpha(1 - \omega_{*\alpha}/\omega)\,\zeta_\alpha Z(\zeta_\alpha)/2R^2, \tag{9b}$$

$$U_1 = 3\omega^2/4v_A^2 + \tau k_\parallel^2/[1 + \zeta_e Z(\zeta_e)], \tag{9c}$$

$k_\parallel$ is the parallel wavenumber, ω is the mode frequency, $\tau = T_e/T_i$, $\omega_* = (mcT/reB)\partial \ell n N/\partial r$, $\zeta_e = \omega/|k_\parallel|v_e$, $\rho_i^2 = T_i M_i (c/eB)^2$, m is the poloidal mode number, Z is the plasma dispersion function, the subscripts refer to electrons, ions and alpha particles, $V_A^2 = B^2/(4\pi N_i M_i)$ is the Alfven speed, $\zeta_\alpha = \omega/|k_\parallel|V_\alpha$, R is the major radius, and $\beta_\alpha = 8\pi N_\alpha T_\alpha/B^2$. If the finite Larmor radius term in the charge neutrality condition is ignored, then Eq. (9a) reduces to the second order eigenmode equation derivable from ideal magnetohydrodynamics. In Eq. (9), we have neglected ω_{*i} and ω_{*e} compared with ω, but $\omega_{*\alpha}$ is kept. Note also that Eq. (9) is applicable to modes with poloidal mode number $m \geq 2$. (The $m = 1$ mode would require full toroidal geometry in the equilibrium.)

When electron damping and alpha particle undamping are ignored, we can derive a quadratic form

$$\omega^2\Big[\int_o^a dr\,\frac{r^3}{V_A^2}\Big|\frac{\partial}{\partial r}\frac{\phi}{r}\Big|^2 + (m^2-1)\int_o^a dr\,|\phi|^2/r\,V_A^2$$

$$-\frac{3}{4}\rho_i^2\int_o^a dr\,r\,V_A^{-2}\Big|\Big(\frac{1}{r}\frac{\partial}{\partial r}r\frac{\partial}{\partial r} - \frac{m^2}{r^2}\Big)\phi\Big|^2\Big]$$

$$= \int_o^a dr\,k_\parallel^2\,r^3\Big|\frac{\partial}{\partial r}\frac{\phi}{r}\Big|^2 + \int_o^a dr(m^2-1)\,k_\parallel^2\,|f|^2/r$$

$$+\rho_s^2\int_o^a dr\,\frac{k_\parallel^2}{r^3}\Big|\frac{\partial}{\partial r}r^3\frac{\ell}{\partial r}\frac{\phi}{r}\Big|^2 + \rho_s^2\int_o^a dr\,k_\parallel^2\,|\phi|^2/r^2$$

$$+2\rho_s^2(m^2-1)\,R_e\Big[\int_o^a dr\,k_\parallel^2\,r^3\Big(\frac{\partial}{\partial r}\frac{\phi^*}{r}\Big)\Big(\frac{\partial}{\partial r}\frac{\phi}{r^3}\Big)\Big] \tag{10}$$

where a is the minor plasma radius, and ρ_s is the ion gyroradius with electron temperature. If $\rho_i/r \ll 1$, $\rho_i\,\partial/\partial r \ll 1$, both sides of Eq. (10) are positive, ω^2 must be positive and the system is neutrally stable. If the finite Larmor radius terms are approximated by their slab form it is impossible to construct a quadratic form, however.

Equation (9) is solved numerically using a conducting wall boundary condition at $r = a$ and $E_r = B_r = 0$ at $r = 0$. For tokamak geometry, $k_\parallel = (m - \ell q)/qR$, where ℓ is the toroidal mode number and q is the safety factor. We assume parabolic profiles for q and the density N, $q(r) = 1 + (q_a - 1)(r/a)^2$, and $N = N_o[\rho_o - (r/a)^2]$

In this paper, we investigate the destabilization of the local Alfven wave $\omega^2 = k_\parallel^2 V_A^2 \equiv \omega_A^2$ due to fast particles by choosing low mode numbers such that the first mode rational surface $k_\parallel = 0$ lies radially outside of the Alfven resonance $U_o = 0$, Eq. (9b). U_o plays the role of a potential well for the radial eigenmodes. For the alpha particles, we assume $\beta_\alpha = \beta_{\alpha o} \exp[-(r/L_\alpha)^2]$ and $N_\alpha = N_{\alpha o} \exp[-(r/L_\alpha)^2]$.

When $\beta_{\alpha o} = 0$, and electron Landau damping is turned off, for fixed ℓ and m such that $k_\parallel \neq 0$ we find radial eigenmodes with purely real ω. The fundamental radial mode has the smallest ω ($\omega/\omega_{Ao} \sim 1$, where ω_{Ao} is the Alfven frequency at the center) and the Alfven resonance surface closest to $r = 0$. As the radial mode number increases, ω increases and the Alfven resonance surface moves outward. When $\beta_{\alpha o} \neq 0$ these eigenmodes are destabilized. Figures 4 show the eigenfunctions of the unstable fundamental and first radial harmonics for the following parameters of an ignited tokamak: $\ell = 3$, $m = 2$, $q_a = 3$, $T_i = T_e = 10$ keV, $B = 45$KG, $N_o = 10^{14}/cm^3$, $\beta_i = \beta_e = 2\%$, $\beta_{\alpha o} = 3\%$, $T_\alpha = 3.5$ Mev, $R = 4m$, $a = 1m$, $L_\alpha = 0.3m$, and $\rho_o = 1.1$.

Analyzing the local dispersion relation obtained from Eq. (9) we see this instability is driven by $\omega_{*\alpha}$. This is numerically confirmed in Fig. 5, where the growth rate $\mathrm{Im}\Omega$ ($\Omega \equiv \omega/\omega_{Ao}$) for the fundamental radial mode is plotted against L_α/a for $T_\alpha = 3.5$, 2.5 and 1 MeV. From Fig. 5, we conclude that i) the growth rate is higher for larger T_α, ii) it increases with decreasing L_α and iii) for fixed T_α, there exists a critical L_α below which the mode is unstable.

As the quantitative results show the conditions for instability are easily met since the alpha particle pressure is localized in the central region. Under these circumstances, quasilinear theory can be expected to flatten the alpha density profile and to yield anomalous outward diffusion of the alpha particle ash.

REFERENCES

[1] LEE, Y. C., et al., Nucl. Fusion 20 (1980) 482.
[2] TANG, W. M., et al., PPPL-1627 (1980).
[3] COPPI, B., et al., Phys. Fluids 10 (1967) 582.
[4] LINSKER, R., in Reversed Field Pinch Theory Workshop, Los Alamos (1980).
[5] KAW, P. K., and GUZDAR, P. N., Comments on Plasma Physics and Controlled Fusion 5 (1980) 189.
[6] EUBANK, H., et al., in Plasma Physics and Controlled Nuclear Fusion Research (IAEA, Vienna, 1979) Vol. 1, P. 167.
[7] KADOMTSOV, B. B., and POGUTSE, O. P., Review of Plasma Physics, Consultant's Bureau, Vol. 5, 249 (1970).
[8] WALTZ, R. E., et al., General Atomic Report GA-A15147 (1978).
[9] PEARLSTEIN, L. D., and BERK, H. L., Phys. Rev. Lett. 23 (1969) 220.
[10] FOST, D. E., et al., in Plasma Physics and Controlled Nuclear Fusion (IAEA, Vienna, 1979), Vol. 1, P. 471.
[11] FRIEMAN, E. A., et al., Phys. Fluids (to be published); HASTIE, R. J., et al., Nucl. Fusion 19 (1979) 1223; CHOI, D. I., and HORTON, W., Phys. Fluids (1980) 356.
[12] CHEN, L., and CHENG, C. Z., PPPL-1562 (1979).
[13] CHEN, L., et al., Nucl. Fusion (to be published).
[14] CHENG, C. Z., and CHEN L., PPPL-1579 (1979).
[15] CHENG, C. Z., and CHEN L., PPPL-1622 (1979).
[16] GUZDAR, P. N., et al., PPPL-1601 (1980).
[17] HASEGAWA, A., and KODAMA, Y., Phys. Rev. Lett. 41 (1978) 1470.
[18] PRATER, R., et al., Phys. Fluids 21 (1978) 434.
[19] CHENG, C. Z., and OKUDA, H., Nucl. Fusion 18 (1978) 587.
[20] OKUDA, H., Phys. Fluids 23 (1980) 498.
[21] ROSENBLUTH, M. N., and RUTHERFORD, P. H., Phys. Rev. Lett 34 (1975) 1428.
[22] HASEGAWA, A., and CHEN, L., Phys. Rev. Lett 35 (1975) 370.

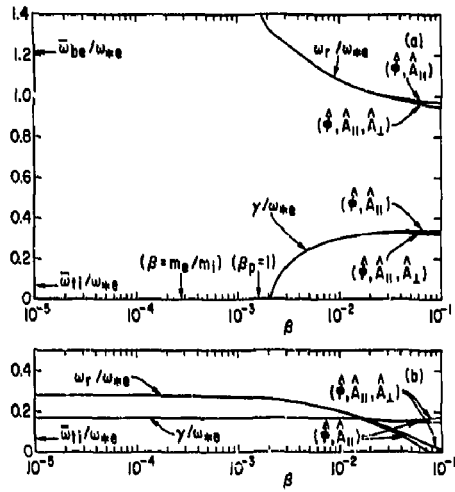

(PPPL-802144)

Fig. 1. $\omega = \omega_r + i\gamma$ versus β for eigenmodes in (a) the shear-Alfvén branch with $\eta_i = \eta_e = -1$, and (b) the drift branch with $\eta_i = \eta_e = 0$.

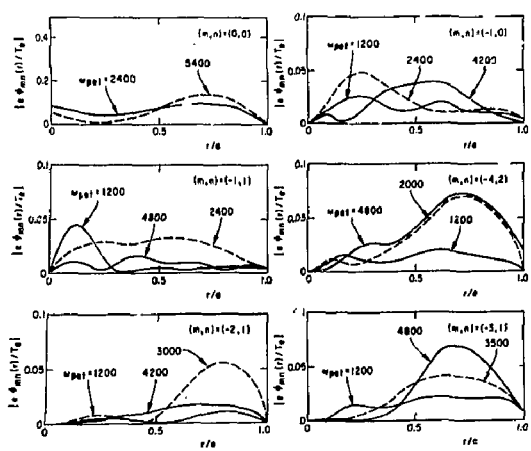

(PPPL-802098)

Fig. 2. Perturbed potentials at different time steps for various (m,n) modes. Here, $q = \sqrt{5}$ is an irrational number.

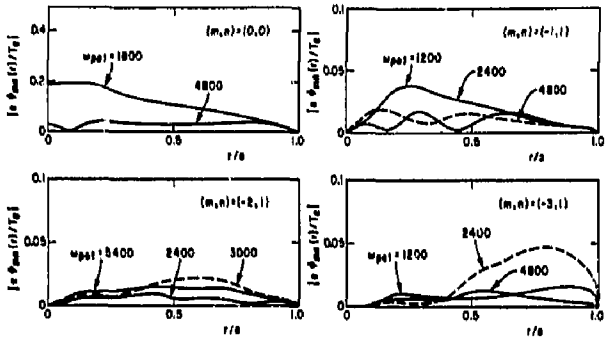

(PPPL-802080)
Fig. 3. Same as Fig. 2., except q = 2 is a rational number.

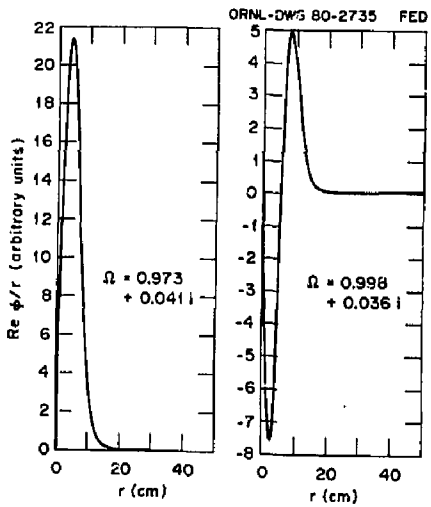

(PPPL-802169)
Fig. 4. Eigenfunctions (Reϕ/r) of the unstable fundamental and first radial harmonics for the parameters of an ignited tokamak given in the text.

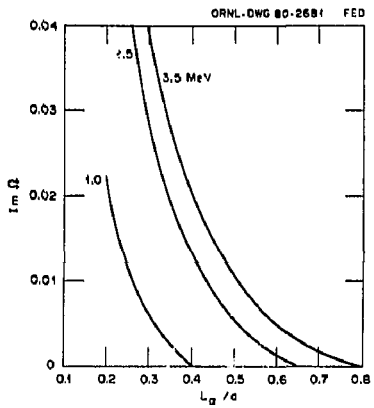

(PPPL-802168)

Fig. 5. Normalized growth rate Im Ω for the fundamental radial mode versus normalized α particle density scale length L_α/a for T_α = 3.5, 2.5 and 1 MeV. Same parameters as in Fig. 4.